Shuttle-Tethered Subsatellite System Stability with a Flexible Massive Tether

P.M. Bainum,* C.M. Diarra,† and V.K. Kumar‡
Howard University, Washington, D.C.

The effect of the in-plane transverse vibrations of a massive, flexible tether on the stability of the Shuttle-tethered subsatellite system about the deployed local vertical orientation is examined analytically and numerically. Within the linear range, the out-of-orbit plane (roll) equation is decoupled from the in-plane swing and extension/contraction modes and has the form of a Mathieu equation. An application of the Floquet theorem shows that parametric instability can result for specific ratios of the tether wave frequency to the orbital rate. In addition, a forced resonance can be further superimposed due to the rotating atmosphere, especially for high-inclination orbits. The divergent time constant can be as small as several orbits for short tether lengths where the subsatellite mass is much less than the tether mass.

I. Introduction

THE Smithsonian Astrophysical Observatory proposed the Shuttle-based "Skyhook" concept consisting of a tether of approximately 100 km length to be deployed from the Shuttle orbiter and transporting at its end a subsatellite experimental package.[1] A subsequent treatment of the dynamics[2] of the Shuttle-tethered subsatellite (STS) system assumed that the motion occurred only within the orbital plane and neglected the tether mass. A tether tension control was proposed such that the tension would vary as a linear function of the tether line length, the length rate, and the commanded (desired) length. The position and velocity control law gains were adjusted according to the frequency of the various system natural modes.[2] A further NASA study covered the three-dimensional dynamics and control, including the inertial effect of the tether mass, aerodynamic forces on the tether and subsatellite, and aerodynamic heating.[3]

Recently, a new tether tension control law (for a massless tether) in which the tension was assumed to vary as a linear function of the difference between the tether line length and the commanded length, the rate of change of the length, the in-(orbital) plane swing angle, and the rate of change of that angle was developed based on linear optimal control theory.[4] During stationkeeping, such a control concept could result in improved transient responses as compared with the previously developed control laws, and the associated tether tension and power levels would not exceed previous requirements. Subsequently, Diarra[5] examined the effects of a massive but taut tether on the dynamics, stability, controllability, and observability of the STS system in its nominal operational stationkeeping mode, using the optimal form of the tether stationkeeping control law.[4] It was found that stability regions previously obtained for the massless tether were now seen to be contracted due to the tether mass.

Misra and Modi studied the general three-dimensional dynamics of the STS system (including rotational motions of the end bodies) where in-plane control of a flexible massive tether was based on a length rate control law.[6] Because of the complexity of the formulation, most of the results were based on numerical simulation techniques.

This paper extends the work of Ref. 5 to examine analytically and numerically the effect of a massive and flexible tether on the stability of the STS system during stationkeeping. The equations of motion are derived using a Newton-Euler formulation. The model includes the effects of gravity and the orbital dynamics.

In order to demonstrate analytically the possibility of parametric instability in the out-of-plane roll motion of the STS system due to (in-plane) transverse tether vibrations, a number of limiting assumptions have been made and will be explained in sequence. More complex formulations, such as provided in Ref. 6, consider more complete flexibility and other effects, with the results obtained based mainly on numerical methods. It is hoped that the results obtained here can provide greater insight into the more comprehensive numerical approaches that will be required to simulate all phases of the actual STS mission.

II. Equations of Motion of the STS System When the Tether Is Massive and Flexible

In this development, the tether is considered massive and flexible with the key elements of the system geometry shown in Fig. 1.

$O'XYZ$ is an Earth-centered inertial reference frame R with $O'Z$ along the Earth's spin axis, $OX_0Y_0Z_0$ is an orbit-fixed reference frame R_0 centered at the center of mass of the Shuttle O with OX_0 along the local vertical and OY_0 along the orbit normal opposite to the orbit angular momentum vector. $Oxyz$ defines the principal axes of inertia $R1$ of the STS system in the undeformed state (not shown).

The system is idealized as two-point masses (the centers of mass of the Shuttle and subsatellite) connected by a massive and flexible homogeneous tether with the Space Shuttle assumed to be moving in circular low-altitude Earth orbit in a spherical gravitational field. The equations of motion are derived using a Newton-Euler formulation. The principal assumptions made in this development are:

1) The Shuttle mass is much greater than the combined mass of the subsatellite and the deployed tether. Hence, the shift in the center mass of the entire system from that of the Shuttle is neglected.

2) The subsatellite is homogeneous, rigid, and spherical and has a small diameter as compared with the tetherline length.

3) At or near the equilibrium position, the tether behaves like a vibrating string, with the amplitudes of the transverse

Received Sept. 2, 1983; revision received Jan. 3, 1984.

*Professor of Aerospace Engineering. Associate Fellow AIAA.

†Graduate Research Assistant, Department of Mechanical Engineering. Student Member AIAA.

‡Senior Graduate Research Assistant. (Presently with Systems and Applied Sciences Corp., Bladensburg, Md.)

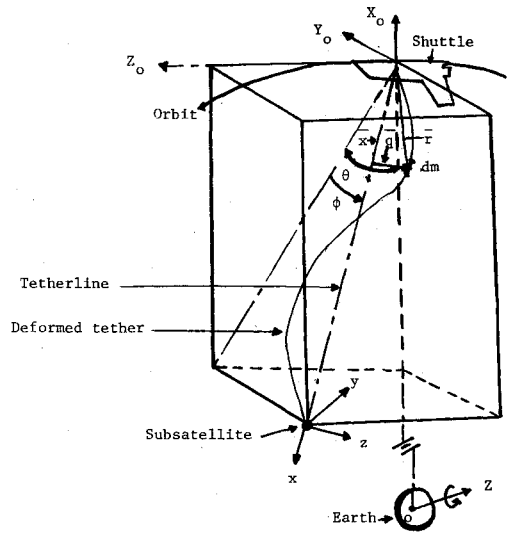

Assumed Euler rotational sequence

$$\begin{bmatrix} x \\ y \\ z \end{bmatrix} = \begin{bmatrix} \cos\phi & \sin\phi & 0 \\ -\sin\phi & \cos\phi & 0 \\ 0 & 0 & 1 \end{bmatrix} \begin{bmatrix} -\cos\theta & 0 & \sin\theta \\ 0 & 1 & 0 \\ -\sin\theta & 0 & -\cos\theta \end{bmatrix} \begin{bmatrix} X_o \\ Y_o \\ Z_o \end{bmatrix}$$

Fig. 1 System (with massive and flexible tether) geometry.

elastic displacements assumed to be small compared with the tether line length.

4) The effects of the twisting motion about the tether line on the system dynamics are neglected.

5) The longitudinal elastic tether displacements are assumed to be negligible.

6) Control is introduced into the system only by modulating the tension level in the tether.

Consider an elemental mass of the system dm having the position vector $\bar{r}$. In the body frame, $R_1(x, y, z)$, see Fig. 1, moving with the tether line $\bar{r}$ can be written as

$$\bar{r} = x\hat{i} + \bar{q} \tag{1}$$

The equation of motion of dm can be expressed by

$$\bar{a} = \bar{f} + L(\bar{q})/\rho + \bar{e} \tag{2}$$

where $\bar{a}$ is the inertial acceleration of dm; $\bar{f}$ the gravitational force per unit mass; $\bar{e}$ the external force per unit mass; $\bar{q}$ the transverse elastic displacement of dm; $x\hat{i}$ the position vector of dm in the undeformed state; L a linear operator that, when applied to the small elastic displacement $\bar{q}$, yields the elastic forces acting on dm; and ρ the mass per unit volume. The expression[7] for $\bar{f}$ contains terms due to gravity at the system center of mass $\bar{f}_0$ and the gravity gradient $M(\bar{r})$,

$$\bar{f} = \bar{f}_0 + M(\bar{r}) \tag{3}$$

With the geometry and Euler angle sequence shown in Figure 1,

$$M = \omega_c^2 \begin{bmatrix} 3\cos^2\phi\cos^2\theta - 1 & 3\sin\phi\cos\phi\cos^2\theta & 3\cos\phi\cos\theta\sin\theta \\ 3\sin\phi\cos\phi\cos^2\theta & 3\sin^2\phi\cos^2\theta - 1 & 3\sin\phi\cos\theta\sin\theta \\ 3\cos\phi\sin\theta\cos\theta & 3\sin\phi\cos\theta\sin\theta & 3\sin^2\theta - 1 \end{bmatrix} \tag{4}$$

where ω_c is the angular velocity of the orbit of the Shuttle center of mass.

Equation (2) can be written in the body frame R_1 as

$$\bar{a}_0 + \ddot{\bar{r}} + 2\bar{\omega}\times\dot{\bar{r}} + \dot{\bar{\omega}}\times\bar{r} + \bar{\omega}\times(\bar{\omega}\times\bar{r}) = \bar{e} + \bar{f} + L(\bar{q})/\rho \tag{5}$$

where $\dot{\bar{r}}$ and $\ddot{\bar{r}}$ are the velocity and acceleration of dm, respectively, in R_1. The inertial angular velocity vector $\bar{\omega}$ can be expressed in terms of the Euler angles and Euler rates in R_1 by

$$\bar{\omega} = (\dot{\theta} - \omega_c)\sin\phi\hat{i} + (\dot{\theta} - \omega_c)\cos\phi\hat{j} + \dot{\phi}\hat{k} \tag{6}$$

After substitution of Eqs. (1) and (3) into Eq. (5) and integrating the result over the entire system (tether and subsatellite), one arrives at the translational equation of motion of the system,

$$\int_m [\ddot{x}\hat{i} + \bar{a}_0 - \bar{f}_0 + 2\bar{\omega}\times\dot{x}\hat{i} + \dot{\bar{\omega}}\times x\hat{i} + \bar{\omega}\times(\bar{\omega}\times x\hat{i}) - M(x\hat{i})]\, dm + \int_m [\ddot{\bar{q}} + 2\bar{\omega}\times\dot{\bar{q}} + \dot{\bar{\omega}}\times\bar{q} + \bar{\omega}\times(\bar{\omega}\times\bar{q}) - M(\bar{q}) - L(\bar{q})/\rho]\, dm = \int_m \bar{e}\, dm \tag{7}$$

In applications, where orbits are circular (or very nearly circular), the term $\int_m (\bar{a}_0 - \bar{f}_0)\, dm$ vanishes.

It should be noted also that, in the rotating body frame R_1,

$$\dot{\bar{r}} = \dot{l}\hat{i} + \dot{\bar{q}} \tag{8a}$$

$$\ddot{\bar{r}} = \ddot{l}\hat{i} + \ddot{\bar{q}} \tag{8b}$$

where l is the base length of the tether and $\dot{l}$ and $\ddot{l}$ the deployment/retrieval rate and acceleration, respectively.

Expression for the Elastic Transverse Displacements

The elastic transverse vibrations can be expanded in series form in terms of a set of admissible functions,[6,8] i.e., for the nth mode,

$$u = \sum_{n=1}^{\infty} \Phi_n(x) A_n(t) \tag{9a}$$

$$v = \sum_{n=1}^{\infty} \Phi_n(x) B_n(t) \tag{9b}$$

where u and v represent displacements along Oz and Oy, respectively.

The functions $\Phi^{(x)}$ can be somewhat arbitrary, as long as they satisfy at least the geometric boundary conditions. It is assumed that at instant $t = 0$ the transverse vibrational velocity $\dot{u}$ is zero and that only the first in-plane mode is excited; thus,

$$u = \sum_{n=1}^{\infty} \Phi_n(x) A_n(t) = \Phi_1(x) A_1(t) \tag{10}$$

A set of admissible functions satisfying both the temporal and spatial boundary conditions, along with the assumption that the elastic displacements occur in the orbital plane, implies

$$\bar{q} = A_0 \cos\omega t \sin(\pi x/l_c)\hat{k} \tag{11}$$

where $\bar{q}$ is the vector displacement of the elastic transverse vibration, k the unit vector along the Oz axis moving with the tether line, A_0 the maximum amplitude the wave can reach, and l_c the desired (commanded) equilibrium base length. If f is the frequency of the wave, then $\omega = 2\pi f$.

Derivation of the System Equations of Motion

In order to have a mathematical description of the system, one should derive three equations describing the motions in the three degrees of freedom of the system. The translational equation of motion is obtained after substituting expressions

from Eqs., (1), (4), (6), (8), and (11) into Eq. (7), integrating it over the entire (tether and subsatellite) system, and taking its projection along the $\hat{i}$ direction. It should also be noted that, in general, $L(\bar{\phi}^{(n)}) = -\rho\omega_n^2\bar{\phi}^{(n)}$ where ρ is the density and $\bar{\phi}^{(n)}$ the nth modal shape vector whose frequency is ω_n.

If $\hat{i}\cdot\int_m \bar{e}\,dm = T_x$, where $\bar{e}$ represents the external forces including those introduced by the controller, m_t the tether mass, ρ_l the tether mass per unit volume, m_s the subsatellite mass, ρ_2 the satellite mass per unit volume, and D the tether diameter, then the translational equation of motion can be written, after evaluation of the various integrals, as

$$(m_s + m_t)\ddot{l} - (m_s + m_t/2)l\left[\dot{\phi}^2 + (\dot{\theta} - \omega_c)^2\cos^2\phi - \omega_c^2(3\cos^2\theta\cos^2\phi - 1)\right] + S_l = T_x \tag{12}$$

where

$$S_l = (4m_t/\pi)A_0(l/l_c)\{-\omega(\dot{\theta} - \omega_c)\cos\phi\sin\omega t + \tfrac{1}{2}\cos\omega t \times[(\dot{\theta} - \omega_c)\sin\phi\dot{\phi} + \omega_c^2 M_{13} + \ddot{\theta}\cos\phi - \dot{\phi}\sin\phi(\dot{\theta} - \omega_c)]\} \tag{13}$$

The equations of rotational motion of the system are obtained by taking the moments of all the external, inertial, and internal forces acting on the system, i.e., from Eq. (7)

$$\int_m \bar{r}x[\bar{a}_0 - \bar{f}_0 + \ddot{\bar{r}} + 2\bar{\omega}x\dot{\bar{r}} + \dot{\bar{\omega}}x\bar{r} + \bar{\omega}x(\bar{\omega}x\bar{r})]\,dm = \int_m \bar{r}x[L(\bar{q})/\rho + M(\bar{r}) + \bar{e}]\,dm \tag{14}$$

The various terms in Eq. (14) can now be evaluated using the techniques of vector calculus. Since the elastic displacements are assumed to be small, only the first-order terms in $\bar{q}$, $\dot{\bar{q}}$, and $\ddot{\bar{q}}$ are retained.

After substituting the values for the integrals in Eq. (14) and taking the projection along the axes $\hat{i}$ and $\hat{j}$, respectively, of R_1, one arrives at the rotational equations for the pitch [Eq. (15)] and the roll [Eq. (16)] as

$$\begin{aligned} &m_s\{l^2[\ddot{\theta}\cos\phi - 2\dot{\phi}\sin\phi(\dot{\theta} - \omega_c) + 3\omega_c^2\cos\phi\cos\theta\sin\theta] \\ &+ 2l\dot{l}\cos\phi(\dot{\theta}\omega_c)\} + m_t\{(l^2/3)[\ddot{\theta}\cos\phi - 2\dot{\phi}\sin\phi(\dot{\theta} - \omega_c) \\ &+ 3\omega_c^2\cos\phi\sin\theta\cos\theta] + \dot{l}\cos\phi(\dot{\theta} - \omega_c)\} + m_t A_0\{[\omega^2(l^2/\pi) \\ &+ \pi(\dot{l}^2/l_c) + 4(\ddot{l}l_c/\pi l) + (l_c/\pi)(\dot{\theta} - \omega_c)^2\sin^2\phi + \dot{\phi}^2(l_c/\pi) \\ &- \omega_c^2(l_c/\pi) + 3\omega_c^2(l_c/\pi)(\sin^2\theta - \cos^2\phi\cos^2\theta] \\ &\times\cos\omega t - 4\omega(\dot{l}l_c/\pi l)\sin\omega t\} = C_y \end{aligned} \tag{15}$$

$$\begin{aligned} &m_s\{l^2[\ddot{\phi} + \sin\phi\cos\phi(\dot{\theta} - \omega_c)^2 + 3\omega_c^2\cos\phi\sin\phi\cos^2\theta] + 2l\dot{l}\dot{\phi}\} \\ &+ m_t\{(l^2/3)[\ddot{\phi} + \sin\phi\cos\phi(\dot{\theta} - \omega_c)^2 \\ &+ 3\omega_c^2\cos\phi\sin\phi\cos^2\theta]\,l\dot{l}\dot{\phi}\} + m_t A_0\{[4(\dot{l}l_c/\pi)(\dot{\theta} - \omega_c)\sin\phi \\ &- \ddot{\theta}(l_c/\pi)\sin\phi - \dot{\phi}l_c(\dot{\theta} - \omega_c)\cos\phi + (l_c/\pi)\dot{\phi}(\dot{\theta} - \omega_c)\cos\phi \\ &+ 3\omega_c^2(l_c/\pi)\sin\phi\cos\phi\sin\theta]\cos\omega t + 2(l_c/\pi) \\ &\times\omega(\dot{\theta} - \omega_c)\sin\phi\sin\omega t\} = C_z \end{aligned} \tag{16}$$

where C_y and C_z are the components of the external torque along the $\hat{j}$ and $\hat{k}$ axis, respectively.

Linearization of the System Equations of Motion

Equations (12), (15), and (16) describe the motion of the STS system for the case where vibrations occur initially only in the orbital plane and where the tether behaves like a vibrating string that has only its first mode excited [the effect of other modes could be modeled by including additional terms in the summation of the series, see Eq. (9)]. During the stationkeeping phase, it is desired to maintain the subsatellite at or close to the nominal equilibrium configuration in which the subsatellite is deployed 100 km below the Shuttle along the local vertical. Hence, the dynamics analysis will be based on a linear model derived from Eqs. (12), (15), and (16) for small values of θ, $\dot{\theta}$, ϕ, $\dot{\phi}$, and $(l - l_c)/l_c$.

Introducing the nondimensional parameters τ and ϵ, where $\tau = \omega_c t$ [$\mathrm{d}(\ )/\mathrm{d}\tau = (\ )'$] and $\epsilon = (l - l_c)/l_c$, and applying "the small angle approximation" to all the expressions containing θ and ϕ in the linear equations, the following approximate linear equations result:

$$\begin{aligned} &\epsilon'' + m_1^*(2\theta' - 3\epsilon) + m_2^*\left(\frac{A_0}{l_c}\right)\left[\left(\frac{4}{\pi}\right)\left(\frac{\omega}{\omega_c}\right)(1 - \theta' - \epsilon)\sin\omega t \right. \\ &\left. + \left(\frac{2}{\pi}\right)(3\theta + \theta'')\right] = \frac{T_x}{l_c\omega_c^2(m_s + m_t)} + 3m_1^* \end{aligned} \tag{17}$$

$$\begin{aligned} &m_s(\theta'' + 3\theta - 2\epsilon') + m_t\left\{\left(\frac{\theta''}{3}\right) + \theta - \epsilon'\right\} + m_t\left(\frac{A_0}{l_c}\right) \\ &\times\left[-\frac{(4\omega)}{\omega_c}\epsilon'\sin\omega t + \frac{(4\epsilon'' - 3)}{\pi}\cos\omega t\right] = \frac{C_y}{l_c^2\omega_c^2} \end{aligned} \tag{18}$$

$$\phi'' + \left[4 - \frac{6A_0}{\pi(3m_s/m_t + 1)}\frac{\omega}{l_c\omega_c}\sin\left(\frac{\omega\tau}{\omega_c}\right)\right]\phi = \frac{C_z}{l_c^2\omega_c^2} \tag{19}$$

where $m_1^* = [m_s + (m_t/2)]/(m_s + m_t)$; $m_2^* = [2m_s + m_t] \div [m_s + (m_t/3)]$

It is seen in Eq. (19) that in the absence of external disturbances C_z, the equation describing the roll motion decouples from the two other equations in the linear range, regardless of the inclusion of the tether mass and flexibility into the system.

III. Effects of Tether Mass and Flexibility on the STS Dynamics

Equation (19) is seen to be in the form of Hill's equation,[9]

$$\phi'' + \left\{4 - \left[\frac{6A_0}{\pi(3m_s/m_t + 1)}l_c\right]\left(\frac{\omega}{\omega_c}\right)\sin\left(\frac{\omega\tau}{\omega_c}\right)\right\}\phi = 0 \tag{20}$$

It is well known that the zero solution of such an equation cannot be asymptotically stable in the Lyapunov sense.

With the aid of the transformation, $\xi = (\Omega\tau/2) - \pi/4$, where $\Omega = \omega/\omega_c$, Eq. (20) may be rewritten as

$$\mathrm{d}^2\phi/\mathrm{d}\xi^2 + [(16/\Omega^2) - (4B_0\cos 2\xi)/\Omega]\phi = 0 \tag{21}$$

where $B_0 = 6A_0/\pi[3m_s/m_t + 1]l_c$.

Equation (21) is now in the canonical form of Mathieu's equation

$$\mathrm{d}^2\phi/\mathrm{d}\xi^2 + (a - 2q\cos 2\xi)\phi = 0 \tag{22}$$

From the Mathieu stability chart,[9] one can obtain the magnitudes of mass ratio m_s/m_t, frequency ratio Ω, and amplitude ratio A_0/l_c that result in system stability. However, for $m_s/m_t = 2$ and $A_0/l_c = 0.01$, values characteristic of the STS system during stationkeeping about the nominally deployed length, $q(\Omega)$ has values for which it is difficult to make an accurate interpretation of the Mathieu chart.

Alternatively, the Floquet analysis[10] can be used to derive the stability conditions on a "point-by-point" basis in parameter space. Equation (20) can be written as

$$\phi'' + p(\tau)\phi = 0 \tag{23}$$

were $p(\tau) = 4 - B_0 \sin\Omega\tau$, with period $T = 2\pi/\Omega$.

By setting $y_1 = \phi$ and $y_2 = \phi' = y_1'$, one could recast Eq. (23) in the following state variable form:

$$\underbrace{\begin{bmatrix} y_1' \\ y_2' \end{bmatrix}}_{y'} = \underbrace{\begin{bmatrix} 0 & 1 \\ -p(\tau) & 0 \end{bmatrix}}_{E(\tau)} \underbrace{\begin{bmatrix} y_1 \\ y_2 \end{bmatrix}}_{y} \tag{24}$$

Assuming that the quantities $Z_{11}(T)$, $Z_{12}(T)$, $Z_{21}(T)$, and $Z_{22}(T)$ are known (where $Z_{ij}(T)$ are the elements of the matrix $[Z(T)]$ that satisfies the matrix equation $[Z(\tau)]' = [E(\tau)][Z(\tau)]$ and that, when $\tau = 0$, equals the identity matrix $[I]$), one can derive the stability conditions by applying the Floquet theorem.[10]

For each set of parameters, a corresponding matrix $[Z(T)]$ can be computed by integrating the matrix equation $[Z(\tau)]' = [E(\tau)][Z(\tau)]$ from 0 to T. The characteristic equation of $[Z(T) - sI] = 0$ is given by

$$s^2 - s\{\text{trace of}[Z(T)]\} + \det[Z(T)] = 0 \tag{25}$$

Since the trace of $E(\tau) = 0$ [in Eq. (24)], an application of the Jacobi-Liouville formula[10] implies that $\det[Z(\tau)] = \det[Z(T)] = 1$. Thus, the eigenvalues of Eq. (25) are given by

$$s_{1,2} = \tfrac{1}{2}\left\{\text{trace}[Z(T)] \pm \sqrt{\{\text{trace}[Z(T)]\}^2 - 4}\right\} \tag{26}$$

We will now examine the following different conditions of the Floquet theorem[10] for this specific application:

1) When the trace of $[Z(T)] > 2$. In this case, the modulus of at least one of the eigenvalues is greater than 1 and the zero solution of Eq. (23) is unstable.

2) When the trace of $[Z(T)] = 0$, $s_1 = -s_2 = i$, and $\|s_i\| = 1$. This corresponds to a set of parameters for which the zero solution is stable.

3) When the absolute value of the trace of $[Z(T)] < 2$. Then, all the eigenvalues are complex numbers with modulus $= 1$, one of which is the conjugate of the other.

4) When the trace of $[Z(T)] = 2$. In this case, the multiplicity $n = 2$. For stability, the nullity k of $[Z(T) - s_n I]$ must be equal to the multiplicity n. Here, $s_n = 1$ $(n = 1, 2)$. The nullity k of $[Z(T) - I]$ is the order of $[Z(T) - I]$ minus the rank of $[Z(T) - I]$. For this problem, the rank of $[Z(T) - I]$ must be zero in order for $n = k$; this can happen only when $[Z(T)] = [I] = [Z(0)]$. We conclude for this second-order system that for the case of multiple roots of the characteristic equation, the stability in the Lyapunov sense is always assured.

IV. Numerical Results

It is seen by examining points on the Mathieu chart in the vicinity of $A_0/l_c = 0.01$ that instability will occur when $a = 4(\Omega = 2)$ and $1(\Omega = 4)$. The resulting stability chart obtained from a point-by-point Floquet analysis (Fig. 2) for $A_0/l_c = 0.01$ corroborates the preliminary results of the Mathieu chart. It can also be seen that, for the number of points analyzed, the instability region around $\Omega = 4$ is larger than the instability region around $\Omega = 2$. (It should be noted that for all the unstable points in the region around $\Omega = 2$, regardless of the mass ratio m_s/m_t, the divergent time constants are very long —on the order of months.)

Figure 3 illustrates the influence of the amplitude ratio A_0/l_c in the presence of parametric instability represented by $\Omega = 4$ for the same initial roll displacement and for the same

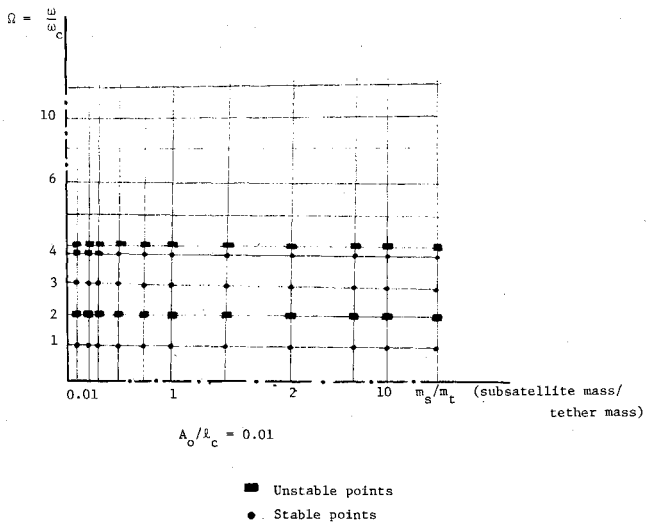

Fig. 2 Stability chart constructed by means of the Floquet theorem.

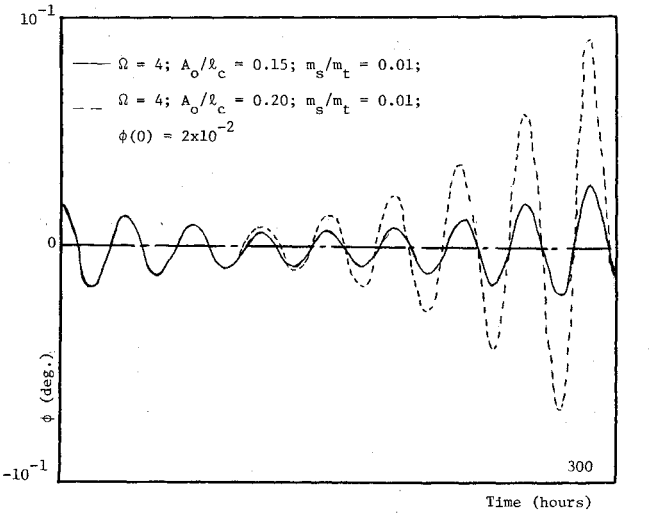

Fig. 3 Parametric instability in the roll degree of freedom.

ratio of m_s/m_t. The increased rate of divergence of roll amplitude for the larger ratio $A_0/l_c = 0.2$ is apparent.

The divergence characteristics predicted from the Floquet analysis are also manifested by the numerically simulated growth of the roll amplitude shown in Fig. 3. In reality, a situation such as depicted by this figure could occur for the STS during stationkeeping about a commanded length representative of the terminal phase of retrieval (or early phase of deployment) with a suitable transverse perturbation in the wave, and for mass ratios that could be realized only if the subsatellite were suddenly severed from the tether, leaving only a small attachment arm connected—i.e., during a possible failure mode where further stationkeeping might be desired in lieu of continuing the deployment (retrieval process). Other results similar to those depicted here with small amplitude ratios and mass ratios corresponding to the fully deployed system for $\Omega = 4$ are characterized by extremely long divergent time constants. It should also be noted (although not illustrated here), that a buildup in roll amplitude, however induced, will eventually lead to instability in the nonlinear equations for the pitch and length degrees of freedom.

In addition to the possibility of system parameters inducing roll instability (parametric resonance), a forced resonance is further superimposed due to the rotating atmosphere, especially for high inclination orbits. As an example, Fig. 4 shows the transient response to an initial 2×10^{-2} deg perturbation

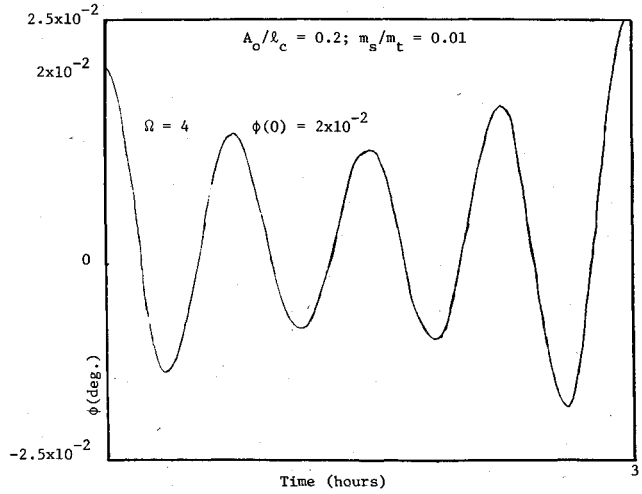

Fig. 4 Parametric and forced resonance in roll due to rotating atmosphere, polar orbit.

in roll for the case where atmospheric effects corresponding to a polar orbit are superimposed for the parameters corresponding to one of the parametric resonance cases of Fig. 3.

(To further dramatize this effect, the drag model here is based on the fully deployed 100 km STS system. It can be seen that under these forced resonance conditions the divergent time constant is two orders of magnitude shorter than that in Fig. 3.)

V. Conclusions

The equation describing the out-of-plane roll motion decouples within the linear range from the length and pitch equations regardless of the presence of tether mass and flexibility in the Shuttle-tethered subsatellite system dynamics. When the frequency of the tether transverse vibration is assumed to be two or four times the orbital frequency, the linear system is unstable. When, in addition to the system parameters inducing roll instability, the drag forces due to a rotating atmosphere are superimposed, the divergent time constant can be shorter than that experienced for the case of parametric instability alone.

The values of the system parameters that yield parametric/forced resonance instability with noticeable divergent time constants correspond to a situation in which the subsatellite mass is two orders of magnitude less than the deployed tether mass—a failure case where most of the subsatellite system would be severed from the tether line. For different applications of tethered connected systems such as in space (platform)-based construction using shorter tethers attached to different size instruments (payloads), this would have to be re-evaluated.

A recommended extension to the present study could consider the stability of the combined pitch and length equations for the linear system, which would necessitate a higher-order Floquet analysis.

References

[1] Colombo, G., Gaposchkin, E.M., Grossi, M.D., and Weiffenbach, G.C., "Shuttle-Born 'Skyhook'. A New Tool for Low Orbital Altitude Research," *Smithsonian Astrophysical Observatory, Reports in Geoastronomy*, No. 1, 1974.

[2] Rupp, C.C., "A Tether Tension Control Law for Tethered Subsatellites Deployed Along the Local Vertical," NASA TMX-64963, 1975.

[3] Baker, W.P. et al, "Tethered Subsatellite Study," NASA TMX-73314, March 1976.

[4] Bainum, P.M. and Kumar, V.K., "Optimal Control of the Shuttle-Tethered-Subsatellite System," *Acta Astronautica*, Vol. 7, May 1980, pp. 1333-1348.

[5] Diarra, C.M., "The Effects of Tether Mass on the Stability and the Controllability of the Shuttle-Tethered-Subsatellite System," AIAA Paper 83-0652, Jan. 1983.

[6] Misra, A.K. and Modi, V.J., "Deployment and Retrieval of a Subsatellite Connected by a Tether to the Space Shuttle," AIAA Paper 80-1693, Aug. 1980.

[7] Santini, P., "Stability of Flexible Spacecrafts," *Acta Astronautica*, Vol. 3, 1976, pp. 685-713.

[8] Xu, D.M., Misra, A.K., and Modi, V.J., "Three Dimensional Control of the Shuttle Supported Tethered Satellite Systems During Retrieval," *Proceedings of 3rd VPI & SU/AIAA Symposium*, Blacksburg, Va., AIAA, New York, 1981, pp. 453-462.

[9] McLachlan, N.W., *Theory of Vibrations*, Dover Publications, New York, 1951.

[10] Cesari, L., *Asymptotic Behavior and Stability Problems in Ordinary Differential Equations*, Academic Press, New York, 1963.